New insights on black carbon in pelagic Atlantic sediments

Kari St.Laurent[1,2], Mark Cantwell[3], Rainer Lohmann[1*]

[1]Graduate School of Oceanography, University of Rhode Island, Narragansett, Rhode Island, U.S.A.

[2]National Oceanic and Atmospheric Administration, National Environmental Satellite, Data and Information Service, Silver Spring, Maryland, U.S.A.

[3]U.S. Environmental Protection Agency, Atlantic Coastal Environmental Sciences Division, Narragansett, Rhode Island, U.S.A.

*Corresponding author: email: rlohmann@uri.edu ; Tel: 401-874-6612; Fax: 401-874-6811

Highlights

- Black carbon comprised 17±6 to 65±18% of the particulate sedimentary organic carbon.
- Black carbon accumulation rates were 6X greater in an aeolian plume compared to a remote site.
- The radiocarbon age was younger in the black carbon fraction compared to the total organic carbon.

Keywords

black carbon; polycyclic aromatic hydrocarbons; radiocarbon; sediments; Atlantic Ocean

Abstract

Black carbon (BC) is ubiquitous in pelagic sediments and presumed to have an older radiocarbon age due to long ocean residence times and pre-aging in terrestrial soils. Here, we analyzed sediments from five regions in the subtropical Atlantic Ocean to quantify the black carbon fraction of the total organic carbon pool. Black carbon, derived from the chemothermal oxidation method, comprised between 17±6% of the sedimentary organic carbon in the Northwest Argentina Basin and 65±18% in the Amazon Delta. Black carbon sediment accumulation rates were six times greater in the Sierra Leone Rise (8.4±4.1 mg cm^{-2} kyr^{-1}) compared to the remote Northwest Argentina Basin (1.3±0.4 mg cm^{-2} kyr^{-1}), possibly due to enhanced regional atmospheric deposition from annual African grassland fires. The radiocarbon age for BC from subtropical Atlantic sediments were more modern compared to the bulk total organic carbon, and BC source was apportioned as biomass burning byproducts from their stable carbon isotopic signatures and characteristic ratios of polycyclic aromatic hydrocarbons. This study demonstrated that subtropical Atlantic Ocean sediments serve as an important sink for young BC.

1. Introduction

Black carbon (BC) is a byproduct of the incomplete combustion of organic matter, including contemporary fossil fuel emissions and both natural and anthropogenic biomass burning (Seiler and Crutzen, 1980; Goldberg, 1985; Schmidt and Noack, 2000, Mitra et al., 2014). Biomass burning events can release large quantities of aerosols, including BC, that can be at magnitudes comparable to modern fossil fuel emissions (Andreae, 1993). The need for a better understanding of BC concentrations, sources, and transport is driven by its implications in climate forcing (Bond and Sun, 2005), its role as a human health hazard (Li et al., 2016), its ability to sorb

53 organic pollutants such as polycyclic aromatic hydrocarbons (Accardi-Dey and Gschwend,
54 2002), and its potential to be a sink for fixed carbon when deposited to remote regions
55 (Kuhlbusch, 1998). Quantifying BC concentrations in remote and understudied regions, such as
56 the pelagic subtropical Atlantic Ocean, could offer insights into the input and accumulation of
57 terrigenous organic matter in an oligotrophic region and assess the relative magnitude of pelagic
58 sediment burial as a sink for BC.
59
60 Black carbon measurements in the environment, however, are complicated by differences in
61 analytical approach, operational definition, recalcitrance, and size of BC particles (Currie et al.,
62 2002; Masiello, 2004; Pohl et al., 2014). Additionally, many marine BC measurements have
63 been performed in near-shore environments or have focused primarily on the Pacific basin,
64 creating a general lack of knowledge of BC sediment concentrations in the remote Atlantic. For
65 example, sedimentary graphitic BC concentrations of 0.14 to 0.65 g_{BC} $kg_{sediment}^{-1}$ have been
66 measured off the Washington U.S. coast using an isotopic approach (Dickens et al., 2004) and
67 BC concentrations ~0.44 g_{BC} $kg_{sediment}^{-1}$ have been measured in the deep Pacific using a chemical
68 oxidation technique (Griffen and Goldberg, 1975). In the remote Pacific Ocean, BC
69 accumulation rates were as low as 0.002 – 0.06 mg cm^{-2} kyr^{-1} and contributed ~15% to the
70 sedimentary organic carbon pool (Griffen and Goldberg, 1975; Suman et al., 1997; Masiello and
71 Druffel, 1998). It is unclear whether BC dynamics are similar in the Atlantic basin. Lohmann et
72 al. (2009) reported that soot carbon, determined by chemothermal oxidation, composed up to
73 34% of the bulk sedimentary organic carbon in the Subtropical Atlantic Ocean. This suggests
74 that pyrogenic carbon inputs could be greater in the subtropical Atlantic region compared to the
75 Pacific.

The subtropical Atlantic Basin in particular could be a potential "hotspot" for atmospheric BC deposition due to intense grass burning events in the African Savanna, anthropogenic activity, and tropical easterly wind patterns favorable for the offshore transport of emission particulates (Cahoon et al., 1992). A previous study reported that BC aerosols from these African grass burning events composed up to 0.8% of the atmospheric particulate matter over the subtropical Atlantic Ocean (Pohl et al., 2014). Aerosols from northern Africa, including grass burning, have been measured as far as the eastern United States coast, demonstrating their long-range transport potential in this region and enhanced atmospheric deposition rate into the subtropical Atlantic Ocean (Perry et al., 1997; Pohl et al., 2014). Likewise, BC atmospheric particulates in Nairobi, Kenya, derived mostly from fossil fuel combustion, were found to exceed the World Health Organization's safe concentration threshold (Kirago et al., 2022a). Recently, BC from savanna grassland burn emissions were found to have a clear interannual variability with stable carbon and radiocarbon isotopes showing significant (≥88%) contributions to the overall biomass burning emissions in Rwanda (Kirago et al., 2022b). It is clear that Africa may be a significant aeolian source of BC deposition to the ocean.

In this study, sediments from the remote Sierra Leone Rise and South Atlantic Ocean, and near-coastal samples from the Senegal, Amazon and Niger Deltas were collected and analyzed with the aims of: 1) determining the concentration of BC using a chemothermal oxidation procedure, 2) contrasting BC accumulation rates in various regions across the subtropical Atlantic, and 3) performing a source apportionment of the BC using radiocarbon, stable carbon isotope measurements and ratios of polycyclic aromatic hydrocarbons (PAHs).

2. Materials and Methods

2.1 Sediment Collection

Shallow sediment samples (≤12 cm) from EN-480-1, EN-480-2, EN-481-7, EN-481-8, and EN-481-9 were collected in the summer of 2010 aboard the *R/V Endeavor* using a 4-barrel multi-corer. Sediment cores were sliced into 1-2 cm sections immediately after recovery. All sediments were stored in pre-combusted (450°C) amber glass jars in a -10°C chest freezer until analysis. Additional sediments from the Department of Geosciences at Bremen University (GeoB cores 4901, 4903, 4905, 4907, 4908, 1701, 9501, and 2814) were also analyzed. These sediment samples were previously collected using multicorer and box corer samplers, sliced into 1-10 cm sections, freeze-dried and ground with a mortar and pestle (Wagner et al., 2004; Zabel et al., 2003).

For this study, the top 10 cm were defined as well-mixed and homogeneous due to bioturbation, thus collectively called the surface sediments. This was supported by qualitatively measuring a suite of organochlorine pesticides, such as dichlorodiphenyltrichloroethane (DDT), which has only been produced since the 1940s (Carvalho et al., 2011), and its breakdown derivatives dichlorodiphenyldichloroethylene (DDE) and dichlorodiphenyldichloroethane (DDD; Supplementary Information). Additionally, a meta-analysis of 791 samples found a global average marine mixed layer depth, due to bioturbation, to be 5.75±5.67 cm for marine sediments (Teal et al., 2008). Lastly, Masiello and Druffel (1998) detected bioturbation up to 12 cm in pelagic Pacific sediments, thus 10 cm was deemed a conservative and appropriate threshold for the depth of the homogenous surface sediment layer.

Sediment cores were grouped into the following regions (with average water depth): Amazon Delta (3140 m; n=4), Niger Delta (2500 m; n=6), Senegal Delta (330 m; n=1), Sierra Leone Rise (3300 m; n=3), and Northwest (NW) Argentina Basin (4950 m; n=1) (Figure 1). We note that samples from the Senegal Delta were shallower (~ 10x) compared to the Amazon Delta and Niger Delta regions.

2.2 Black Carbon Methodology

Sedimentary BC concentrations were quantified using chemothermal oxidation and petrographic analysis (Table 1). The chemothermal oxidation at 375°C (BC_{CTO}) method relies on the thermal stability of soot-like carbonaceous particles to isolate the BC fraction but will oxidize charcoal-like BC along with the organic carbon fraction (Gustafsson et al., 1997; Elmquist et al., 2004). For the purpose of this study, the BC fraction derived by chemothermal oxidation was considered as soot-like black carbon as suggested by the BC combustion continuum (Masiello, 2004). All sediments were decalcified using 10% hydrochloric acid, added until effervescence ceased, dried slowly at 35°C, and homogenized with a mortar and pestle.

Briefly, 10% hydrochloric acid was added dropwise to sediments dampened with Milli-Q water until effervescence ceased, similar to Lohmann et al. (2009). A thin layer of ~5 mg of sediment was combusted at 375°C with a steady stream of high purity compressed air for 24 hours to isolate the BC_{CTO}. Sediment samples from the GeoB cores were quantified using an Elementar Vario MICRO cube elemental analyzer coupled to an Isoprime100 isotope ratio-mass spectrometer (IR-MS); sediments collected on EN-480 and EN-481 were analyzed on a Carlo

Erba elemental analyzer coupled to a GV Optima 588 system IR-MS. The detection limit of both instruments was 100 ng of carbon. A portion of the decalcified sediment, prior to the chemothermal oxidation, was reserved to measure the bulk sediment total organic carbon (TOC) on the same instrumentation listed above. Hereafter, organic or black carbon concentrations will be reported as the fraction of carbon (TOC or BC) in that sample as $g_C\ kg_{sed}^{-1}$ where kg_{sed}^{-1} is carbonate free sediments.

Additionally, a petrographic analysis was performed on sediment samples from the EN-480 (Amazon Delta) and EN-481 (Sierra Leone Rise) expeditions ($BC_{optical}$). Approximately 50 g of sediment from the Amazon Delta (sediment depths 0-6.0, 5.5-9, and 8.5-12.0 cm) and Sierra Leone Rise (0-4.0 and 4.0-8.0 cm) were analyzed quantitatively using microscopy by Dr. Bertrand Ligouis at the Laboratories for Applied Organic Petrology at the University of Tübingen, Germany. Briefly, polished sediments were observed under a Leitz DMRX-MPVSP microscope photometer using a magnification up to 500X with reflected white light, uv fluorescence, plane-polarized light, and cross-polarized light (Taylor et al., 1998; Crelling et al., 2006). Various anthropogenic and natural organic matter fragments were detected including char, soot, coal, plastic, pollen, and fungal spores (see Supplementary Information).

2.3 Sedimentation Rate Estimates

Sedimentation rates were obtained by using published data from an existing data base to calculate the BC and PAH fluxes to the ocean floor (Table 2). Sedimentation rates for all regions were estimated using published data from the www.pangaea.de global inventory. If there was no published data for a specific core used in this study, the averaged sedimentation rates of nearby

sites were used as an approximation. Black carbon accumulation rates were estimated as the product of the BC_{CTO} concentration, the regional sedimentation rate, and the dry bulk density (DBD). The DBD was approximated using volume-calibrated ceramic crucibles to determine the dry mass per volume of the homogenized sediments similar to St.Laurent et al., (2020).

2.4 Radiocarbon Analysis

Radiocarbon was measured in surface sediment samples from the Amazon Delta (EN-480; Core 1a; 0-6 cm; n=5) and Sierra Leone Rise (EN-481; Core 9a; 0-5 cm; n=5) regions at the National Ocean Sciences-Accelerator Mass Spectrometry (NOSAMS) facility at Woods Hole Oceanographic Institute using the 'reconnaissance' method. This rapid analysis method was initially developed to quickly and cheaply quantify radiocarbon in corals by reducing organic matter into graphite before radiocarbon analysis on a continuous-flow accelerated mass spectrometer (Burke et al., 2010; McIntyre et al., 2011). Briefly, both TOC (~0.10 to 0.35 mgC) and BC_{CTO} (~0.15 to 0.80 mgC) samples were combusted into carbon dioxide using a modified elemental analyzer and then converted to graphite using a zinc reduction method before analysis (Xu *et al.*, 2007).

While the reconnaissance method offers a reasonable number of samples to be prepared and processed quickly, it is less precise than traditional analytical approaches (Burke et al., 2010). However, for the purpose of this study, the accuracy of the data was within an acceptable range (1.0403±0.0050 fraction modern, expected 1.0398) as determined by oxalic acid standards compared to the continuous-flow mass spectrometer. The instrumental standard deviation for the sediment samples was 20-30 ^{14}C years for both TOC and BC_{CTO}. Here, we report the radiocarbon

values as the blank-corrected fraction modern (Fm_c) and as ^{14}C years as described by Burke et al. (2010).

2.5 Polycyclic Aromatic Hydrocarbon Analysis

Black carbon sources were assessed using $\delta^{13}C$ and select polycyclic aromatic hydrocarbons (PAHs). $\delta^{13}C$ values were determined alongside the chemothermal oxidation method via IR-MS. For the PAH analysis, homogenized sediments were extracted with an accelerated solvent extractor (Dionex ASE 350) in 6 cycles at 150°C using a 50/50 mix of hexane and acetone. Prior to extraction, d_{10}-acenapthene, d_{10}-phenanthrene, d_{12}-chrysene, and d_{12}-perylene were added to each sample to assess recovery. Solvent extracts were evaporated to 1 mL using a rotary evaporator and purified through a column containing 2 mg of activated silica with 45 mL of a 30/70 solvent mixture of dichloromethane and hexane. Extracts were evaporated with N_2 gas to 50 µL and an injection surrogate of p-terphenyl was added before analysis on an Agilent 6890 Series gas chromatograph coupled to a 5973 Mass Selection Detector (GC-MS). All samples were quantified using ChemStation software. The following 24 PAHs were measured: napthalene, 2-Methyl napthalene, acenapthylene, acenapthene, biphenyl, 1,5-dimethyl napthalene, flourene, 2,3,5-trimethyl napthalene, phenanthrene, anthracene (An), 2-methyl flourene, dibenzothiophene, 1-methyl phenanthrene, 9-methyl anthracene, fluoranthene (Fl), pyrene (Py), 4,5-dimethyl phenanthrene, 3,6-dimethyl phenanthrene, 1-methyl pyrene, retene, perylene, benzo(g,h,i)perylene (Bghi), indeno(1,2,3-c,d)pyrene (IP), dibenzo(a,h)anthracene. Source apportionment was assessed on all surface sediments using three PAH ratios as described in Yunker et al. (2002).

2.6 Quality Control and Assurance

The standard reference materials (SRMs) 1941b (marine sediment), 1650 (diesel soot), 1649a (urban dust), mollisol (chernozem soil), risotto char, and sand (methodological blank) were quantified alongside all sediments for BC_{CTO} as recommended by the BC ring trial (Hammes et al., 2007). The analytical average and expected range, respectively, for these SRMs using the chemothermal oxidation method (BC_{CTO}) were: 1941b (our average 0.51%; inter-laboratory range: 0.38-0.74%), 1649a (1.49%; 0.9-2.59%), mollisol (0.11%; 0.0-0.44%), risotto char (0.9%; 0-2.1%), and 1650 (43.2%; 32.5-44.0%). Our BC_{CTO} results are well within the values reported by Hammes et al., (2007). No BC was detected on the sand blank.

For the ASE extractions, a blank cell using Fisher Scientific sea-washed sand was used for every 5 sediment samples. Recoveries of internal surrogates were between 50-99% for all PAHs. Blank ΣPAH concentrations averaged 2.6 ng/g and were detected at a level of less than 4.5% of the smallest ΣPAH sample.

2.5 Data Analysis

All calculations and statistical analyses were conducted using R version 4.1.1. A Shapiro-Wilks test was used to test for normality. If data were considered to not be normally distributed, differences were calculated using a pairwise Wilcoxon Test with a Bonferroni correction. Significance was determined when the p-value was <0.05. Upcore trends were assessed using a Pearson's product-movement correlation test using the cor.test() function in R (version 4.3.1).

3. Results

3.1.1 Surface Sediment Carbon Concentrations

Surface sediment BC_{CTO} concentrations, averaged by region, were greatest in the Senegal Delta (7.7±0.4 gC kg^{-1}; n=6) and Niger Delta (7.4±2.4 gC kg^{-1}; n=77) and lowest in the NW Argentina Basin (1.1±0.3 gC kg^{-1}; n=8; Table 1; Figure 2). The Sierra Leone Rise, located approximately 1000 km from the NW African Coast, had a greater BC_{CTO} surface sediment concentration (6.5±3.1 gC kg^{-1}; n=64) compared to the Amazon Delta (4.1±1.4 gC kg^{-1}; n=48) which is located approximately 800 km from the Amazon River's interface into the Atlantic.

Total organic carbon surface sediment concentrations were greatest in the Senegal Delta (22.0±1.0 gC kg^{-1}; n=6), Niger Delta (15.9±6.1 gC kg^{-1}; n=77), and Sierra Leone Rise (15.4±3.4 gC kg^{-1}; n=58), and comparatively lowest in the NW Argentina Basin (7.0±0.9 gC kg^{-1}; n=10) and Amazon Delta (6.4±1.8 gC kg^{-1}; n=45). The BC_{CTO} fraction of the bulk total organic carbon (TOC) was highly variable with the greatest ratio in the Amazon Delta (65±18%; n=45) and lowest ratio in the NW Argentina Basin (17±6%; n=8).

Both the Amazon Delta and NW Argentina Basin were found to have statistically unique BC_{CTO} concentrations while the BC_{CTO} concentrations were not significantly different between the Niger Delta, Senegal Delta, or Sierra Leone Rise (Figure 2; pairwise Wilcoxon test with the Bonferroni correction method). Surface sediment TOC concentrations were not significantly different between the Niger Delta and Sierra Leone Rise, nor between the Amazon Delta and

NW Argentina Basin. For the ratio of BC/TOC, the following pairs were considered not to be significantly different: the Amazon Delta and the Niger Delta, the NW Argentina Basin and the Senegal Delta, and the Senegal Delta and the Sierra Leone Rise (Table 1).

3.1.2 Petrographic Analysis

Anthropogenic particles were detected in the sediments analyzed from the Amazon Delta (0-9 cm) and Sierra Leone Rise (0-9 cm) by an optical-based petrographic analysis (Table 1). Soot, possibly from traffic combustion (size fraction 3-60 and 3-100 μm for the Amazon Delta and Sierra Leone Rise, respectively), was the dominant form of anthropogenic $BC_{optical}$, followed by plastic and char from coal combustion (Sierra Leone Rise only). The $BC_{optical}$ abundance for the surface Amazon Delta sediments (0-6 cm) ranged from 0.4 to 1.7% using an effective soot density of 0.5 g cm^{-3} (Gysel et al., 2011). The Sierra Leone Rise contained both soot particles (0.4 to 1.7%) and charcoal particles (0.06 to 0.11%) derived from coal combustion, resulting in a $BC_{optical}$ concentration range between 0.5 to 1.8%.

3.2 Upcore Black Carbon Concentrations

Black carbon concentrations did not vary greatly with depth (Figure 3) which could be indicative of constant BC inputs over the chronologic period as represented by the sampling depth. We note that our regions had different sampling resolutions (e.g. depth interval of sampling and core length) but believe these data help depict the upcore variability of the sedimentary organic carbon. As the data were highly variable, our interpretation is mostly qualitative to describe general patterns and trends. The Amazon Delta was the only region with a visibly increasing trend of BC_{CTO} concentration upcore (R^2=0.47; p-value<0.05). The Senegal Delta region also had an increasing upward trend (R^2=0.53; p-value<0.05) which could be an artifact of the small

sample size (5 sampling intervals). The Sierra Leone Rise (R^2=0.05; p-value=0.72), Niger Delta (R^2=0.06; p-value=0.55), and NW Argentina Basin (R^2=-0.02; p-value=0.90) had no general upcore trends of BC_{CTO} concentrations and displayed the greatest variability near the surface.

The Niger Delta had the greatest BC_{CTO} variability across all sampled depths. This region had the greatest number of cores, all with varying distances to the mouth of the Niger River (Figure 1) which resulted in high regional variability. For example, the top 10 cm of the Niger Delta region has a range of surface BC_{CTO} concentrations from 1.7 to 11.4 gC kg^{-1}. Both the Senegal Delta and NW Argentina Basin displayed fairly stable upcore patterns (Figure 3).

3.3 Carbon Source Assessment

3.3.1 Stable Carbon Ratios

The general $\delta^{13}C$ range of organic material from the C_3 carbon fixation pathway is -23 to -28‰ while the C_4 fractionation is more enriched between -12 to 16‰ (Farquhar et al., 1989). Despite C_4 biomass comprising only ~13% of modern-day plant metabolism, the Subtropical Atlantic receives significant C_4 material inputs from African Savanna grasses delivered by the easterly winds (Cahoon et al., 1992; Cerling et al., 1993). Additionally, the typical $\delta^{13}C$ range for marine plankton is estimated between -19 and -22‰ (Holtvoeth et al., 2003); benthic foraminifera from the genus *Cibicides,* a common paleotracer, globally have a $\delta^{13}C$ range between -0.7 to 1.9‰ (Schmittner et al., 2017), and petroleum sources including crude oil (-23.3 to -32.5‰) and gas (22.6 to 23.2‰) display wide ranges depending on region (Yeh and Epstein, 1981).

The bulk TOC-$\delta^{13}C$ values for the Atlantic surface sediments (Table 3) were broadly within the signature for marine plankton between -19 and -22‰ (Holtvoeth et al., 2003) with a study wide average of -19.1±1.9‰ (range of -15.3‰ in the Sierra Leone Rise to -23.5‰ in the Niger Delta). The $\delta^{13}C$-BC_{CTO} had a range of mean values: -28.3±4.6‰ (Amazon Delta; n=48), -23.9±4.6‰ (Niger Delta; n=77), -21.2±3.1‰ (Senegal Delta; n=6), -23.2±4.6‰ (Sierra Leone Rise; n=63), -25.4±1.5‰ (NW Argentina Basin; n=8). Bulk TOC-$\delta^{13}C$ values were comparatively more enriched than the $\delta^{13}C$-BC_{CTO} for these regions.

A mass balance to estimate the OC-$\delta^{13}C$ values was conducted by applying equation 1. The thermally labile $\delta^{13}C$-OC fraction was estimated using the regional average BC_{CTO}, OC, and TOC concentrations and the $\delta^{13}C$ values for BC_{CTO} and TOC:

$$\delta^{13}OC = \frac{([TOC]*\delta^{13}TOC)-([BC]*\delta^{13}BC)}{[OC]} \qquad \text{eq 1.}$$

The average regional $\delta^{13}C$-OC values were -6.0‰ (Amazon Delta), -14.0‰ (Niger Delta), -18.8‰ (Senegal Delta), -12.8‰ (Sierra Leone Rise), and -22.5‰ (NW Argentina Basin).

3.3.2 Polycyclic aromatic hydrocarbons

The concentration of ∑PAHs in surface sediments (Table 3) was greatest and most variable in the Niger Delta (14.12±24.21 μgPAH g^{-1}; n=38) and lowest at the Sierra Leone Rise (1.13±0.89 μgPAH g^{-1}; n=18). Unexpectedly, ∑PAH was greater at the remote NW Argentina Basin (3.84±4.05 μgPAH g^{-1}; n=5) compared to the Amazon Delta (1.93±0.94 μgPAH g^{-1}; n=19) and similar to the Senegal Delta (3.87±2.31 μgPAH g^{-1}; n=3). The elevated ∑PAH concentrations for the NW Argentina Basin were mostly due to variable contributions from indeno(1,2,3-c,d)pyrene (IP; 45.2±42.6%) and benzo(g,h,i)perylene (Bghi; 6.7±15.0%). Both IP and Bghi were also large

components of the surface sediment ∑PAH concentrations for most regions, including the Amazon Delta (IP=40±21%; Bghi=31±20%), Sierra Leone Rise (IP=37±12%; Bghi=52±16%), Niger Delta (IP=19±24%; Bghi=40±32%), and Senegal Delta (IP=18±15%; Bghi=8±8%). This is consistent with findings from a previous study (Pikkarainen 2004).

Ratios of select PAHs were used to apportion source in the surface sediments as described by Yunker et al., (2002; Figure 4). Approximately 97% of sediments extracted for PAHs were apportioned as combustion-derived using the ratio of anthracene (An) to the sum of PAHs with a molecular weight of 178 g mol^{-1} (An + phenanthrene). The ratios of fluoranthene (Fl)/FL+Pyrene(Py) versus IP/IP+Bghi indicated that ~25% of the PAHs extracted from these sediments were apportioned as grass, wood, and/or coal combustion, with the majority of those samples located in the Amazon Delta. Up to 58% of the samples could be apportioned as biomass burning. The Niger Delta was unique in that petroleum combustion and/or petroleum were the most likely source.

3.3 Black carbon and polycyclic aromatic hydrocarbon accumulation rates in pelagic sediments

The greatest average BC_{CTO} accumulation rates were derived for the Senegal Delta (41.6±2.2 $mgBC_{CTO}$ cm^{-2} kyr^{-1}; n=6) and Niger Delta (24.6±8.0 $mgBC_{CTO}$ cm^{-2} kyr^{-1}; n=77) while the lowest BC_{CTO} accumulation rates were found in the Amazon Delta (2.9±1.0 $mgBC_{CTO}$ cm^{-2} kyr^{-1}; n=48) and NW Argentina Basin (1.3±0.4 $mgBC_{CTO}$ cm^{-2} kyr^{-1}; n=8 Table 2). BC_{CTO} accumulation rates were 8.4±4.1 $mgBC_{CTO}$ cm^{-2} kyr^{-1} (n=64) in the remote Sierra Leone Rise. $BC_{optical}$ accumulation rates for the Amazon Delta (range 2.8-12.1 $mgBC_{CTO}$ cm^{-2} kyr^{-1}; n=3) and

Sierra Leone Rise (6.6-23.8 mgBC_{CTO} cm^{-2} kyr^{-1}; n=2) were comparable to the BC_{CTO} accumulation rates.

Accumulation rates of ∑PAHs in this study ranged from 1.4±0.7 μgPAH cm^{-2} ky^{-1} (n=19) in the Amazon Delta region up to 47.0±80.6 μgPAH cm^{-2} ky^{-1} (n=38) in the Niger Delta. Both the Niger Delta and Senegal Delta (20.9±12.5 μgPAH cm^{-2} ky^{-1}; n=3) had the greatest ∑PAH accumulation rate.

3.4 Sedimentary radiocarbon assessment

The BC_{CTO} in Amazon Delta (Fm_c=0.95±0.01; 450±40 ^{14}C years) and Sierra Leone Rise (Fm_c=0.88±0.05; 1030±500 ^{14}C years) sediments were younger than the corresponding bulk sedimentary TOC in the Amazon Delta (Fm_c=0.77±0.01; 2130±110 ^{14}C years) and Sierra Leone Rise (Fm_c=0.83±0.02; 1520±200 ^{14}C years). The CTO_{BC} and TOC were found to be significantly different for the Amazon Delta using paired sample t-test ($p<0.05$) but not for the Sierra Leone Rise ($p = 0.11$). We note, however, the limited sample size and lower precision from the reconnaissance method (Burke *et al.*, 2010).

4 Discussion

4.1 The ubiquity of black carbon

Black carbon was ubiquitous in all subtropical Atlantic sediments collected in this study, regardless of distance from continental emissions or river input. For example, BC was detected at the NW Argentina Basin, our most remote site, which is ~1400 km from the Southeast coast of

South America, >1800 km from the mouth of the closest tributary (the Paraná River), and not impacted by any major atmospheric emission plumes. The NW Argentina Basin BC_{CTO} concentration was 1.1±0.3 g_{BC} kg_{sed}^{-1}, which is comparable to other pelagic sites in both the Atlantic and Pacific Oceans; for example, 1.0-3.4 g_{BC} kg_{sed}^{-1} off the Swedish Continental Shelf (chemothermal oxidation at 375°C; Sanchez-Garcia et al., 2012), 0.4-1.0 g_{BC} kg_{sed}^{-1} off the South American Coast (chemothermal oxidation at 375°C; Lohmann et al., 2009), 2.2-6.3 g_{BC} kg_{sed}^{-1} off the Iberian Margin (chemothermal oxidation at 375°C; Middelburg et al., 1999), and 0.4-1.6 g_{BC} kg_{sed}^{-1} off the Iberian Margin (chemical oxidation via HNO_3; Middelburg et al., 1999). Although BC is a minor fraction of the overall global carbon budget, the recalcitrance and ubiquity of BC in sediments renders it a potential carbon sink, effectively removing biogenic carbon on long-term timescales (Kuhlbusch and Crutzen, 1995).

Similarly, BC has been found to comprise significant portions of the total sedimentary organic matter pool in the pelagic ocean. Previous studies have found BC to comprise 12-31% of the total organic carbon pool in the Pacific Ocean abyssal plain (chemical treatment via $H_2Cr_2O_7$ + H_2SO_4; Masiello and Druffel, 1998;), 15.8% ±0.09% in global riverine systems (benzene polycarboxylic acid method; Coppola et al., 2018), 16-61% in the North Sea (chemothermal oxidation at 375°C and chemical treatment via HNO_3; Middelburg et al., 1999), and 3-34% in pelagic Atlantic Ocean sediments (chemothermal oxidation at 375°C; Lohmann et al., 2009).

However, our ranges in fluvial and pelagic Atlantic sediments suggest that BC_{CTO} comprised significant portions of the sedimentary total organic matter pool, with BC_{CTO} fractions being ~4 times greater in fluvial Amazon sediments and ~6 times greater in the Sierra Leone Rise

compared to the remote NW Argentina Basin. This supports that aeolian deposition likely played an important role in delivering BC to remote sediments in this study area. In this paper, we focused solely on the particulate BC; we note that dissolved black carbon and future feedbacks between climate, wildfires, and BC transport should be further explored (Coppola et al., 2022).

Caution should be applied when comparing black carbon concentrations reported in previous studies since different methodologies measure different portions of the BC combustion continuum (Masiello, 2004); sedimentary BC concentrations and BC/TOC ratios may vary by study depending on the analytical method used. In this study, we applied the chemothermal oxidation at 375°C (CTO-375) approach which operationally isolates the more recalcitrant soot-like BC particulates while oxidizing thermally labile organic carbon which may include char and charcoal-like BC (Forbes et al., 2006). Since the CTO-375 detects only the most thermally recalcitrant BC fractions, the values reported by this study are likely conservative estimates.

4.2 Export of black carbon and polycyclic aromatic hydrocarbons to deep marine sediments

The Subtropical Atlantic Ocean, even the remote areas removed from direct fluvial inputs, displayed measurable accumulation rates of BC_{CTO} and PAHs. Black carbon and combustion-derived PAHs originate from terrestrial processes; thus these accumulation rates represent an export of carbonaceous and hydrocarbon materials from land and the atmosphere to deep sea sediments. Accumulation rates of BC_{CTO} using sedimentation rates from previously published studies ranged from 1.3±0.4 mgBC cm^{-2} kyr^{-1} in the NW Argentina Basin up to 41.6±2.2 mgBC cm^{-2} kyr^{-1} in the Senegal Delta (Table 2). This range is comparable and/or elevated to the U.S.

Washington Coast (1.5-3.1 mgBC cm^{-2} kyr^{-1}; chemothermal oxidation at 375°C and chemical treatment; Dickens et al., 2004), African Coast (0.5-7.8 mgBC cm^{-2} kyr^{-1}; chemothermal oxidation at 375°C Lohmann et al., 2009), and the pelagic Pacific (0.002-3.6 mgBC cm^{-2} kyr^{-1}; synthesis of multiple methods; Suman et al., 1997).

The approximate age of the surface sediments (top 10 cm) analyzed in this study, using the literature-derived deposition rates, are 2.0 kyr (Niger Delta), 2.9 kyr (Senegal Delta), 3.3 kyr (Sierra Leone Rise), 9.2 kyr (Amazon Delta), and 13.2 kyr (NW Argentina Basin). We hypothesize that biomass burning is a primary source of BC and that inputs have been fairly stable for millennia with some observations of recent increases. This is supported by the PAH ratios (Table 3) which suggests the dominance of biomass combustion source of grass, wood, or coal combustion for all sites. A biomass burning source is further inferred by the $\delta^{13}C$ signal suggesting contributions from C_4 plant inputs, such as those from Savanna grasses.

Black carbon accumulation rates derived from the petrographic analysis in the Amazon Delta and Sierra Leone Rise mostly agreed with the BC_{CTO} quantification method (Table 2). In the Amazon Delta, the $BC_{optical}$ accumulation rate ranged from 2.8 to 12.1 mg cm^{-2} kyr^{-1} and was 2.9±1.0 mg cm^{-2} kyr^{-1} for the BC_{CTO} accumulation rate. The $BC_{optical}$ accumulation rate from the Sierra Leone Rise also agreed with the BC_{CTO} accumulation rate at a range of 6.6 to 23.8 and 8.4±4.1 mg cm^{-2} kyr^{-1}, respectively. For the $BC_{optical}$ accumulation rates, it is notable that the Sierra Leone Rise has a ~2 times greater accumulation rate compared to the Amazon Delta. This finding is consistent with expectations that the easterly trade winds transport large quantities of terrestrial particles to the Subtropical Atlantic Ocean (Pohl et al., 2014).

∑PAHs in deep sea sites off the Mississippi River Delta ranged from 1.72 to 51.14 μgPAH cm^{-2} ky^{-1} (Adhikari et al., 2016) and remote sediments off the U.S. Northeast had individual PAH deliveries consistently near 1 μgPAH cm^{-2} ky^{-1} and averaged 35 μgPAH cm^{-2} ky^{-1} closer to urban areas (Gschwend and Hites, 1981). Comparisons of ∑PAH accumulation rates can be challenging since many studies often measure different analytes. However, here we show that ∑PAHs can accumulate in remote pelagic sediments in high rates. In the Niger Delta, PAH ratios indicated petrogenic source, which is in-line with the known oil production in that region (Elum et al., 2016).

4.3 The importance of atmospheric deposition and biomass burning emissions

The Sierra Leone Rise (Figure 1) is one of the shallowest parts of the abyssal Atlantic basin (site depth 3300 m) and is situated directly within the African emissions plume which transports large quantities of organic aerosols from the annual dry season grassland burnings due to southeasterly trade winds (Cahoon et al., 1992; Perry et al., 1997; Pohl et al., 2014). Black carbon from sub-Saharan Africa were dominated by biomass burning emissions (93±3%), and BC particulates were composed equally of C_3 and C_4 plants (Kirago et al., 2022). An enhanced deposition of pyrogenic materials in this region is also consistent with previous buoy-based measurements which found 2.4 gBC kg^{-1} and a BC/TOC percent ratio of 24% (Eglinton et al., 2002). These materials were hypothesized to originate from Northwest Africa due to atmospheric patterns transporting burn emission to the Subtropical Atlantic Ocean.

Both the Sierra Leone Rise and NW Argentina Basin are classified here as remote sites (>800km from the nearest continent). The NW Argentina Basin was expected to have the lowest BC_{CTO} accumulation rate as there are no riverine inputs and synoptic atmospheric patterns are unfavorable for substantial atmospheric inputs; BC_{CTO} accumulation rates measured in this study were comparable to soot-like BC accumulation rates measured in open ocean and margin sediments, where soot-like denotes a chemothermal oxidation BC method was applied (Suman et al., 1997; Lohmann et al. 2009). Thus, the NW Argentina Basin could represent a useful reference site for BC_{CTO} accumulation in pelagic sediments removed from the Aeolian plume of terrestrial particles originating from the African continent (Pohl et al., 2014; Kirago et al., 2022). The enhanced accumulation rates of soot-like BC (Table 2) to the Sierra Leone Rise (8.4±4.1 $mgBC_{CTO}$ cm^{-2} kyr^{-1}) were up to six times greater than the NW Argentina Basin sediment region (1.3±0.4 mgBC cm^{-2} ky^{-1}).

Both the elevated TOC and BC_{CTO} accumulation rates in the Sierra Leone Rise, compared to the NW Argentina Basin, are presumably from atmospheric deposition originating from Savanna grassland burn emissions (Eglinton et al., 2002; Pohl et al., 2014; Kirago et al., 2022). This is supported by the more enriched $\delta^{13}C$-TOC found at the Sierra Leone Rise (-17.2±1.2‰) compared to the NW Argentina Basin (-22.6±0.9‰), which suggests an input of C_4 materials, such as Savanna grasses. Easterly trade winds in combination with interannual grassland burning events thus makes remote sites within sub-Tropical Atlantic Ocean prone to elevated aeolian deposition of TOC and BC compared to other marine basins such as the Pacific. The $\delta^{13}C$ values we report for both TOC and BC_{CTO} are consistent and similar to those reported in South Atlantic sediments by Lohmann et al., 2009.

We recognize that the derived δ^{13}C-OC fraction of our data are highly enriched (eq. 1), particularly for the Amazon Delta (-6.0‰). This indicates that the Amazon Delta region was distinctly separate from the other regions analyzed in this study and it could indicate that we had a fraction of recalcitrant carbonates or petroleum included in the sediments (despite our rigorous acidification process to remove the inorganic carbon fraction). The general trends for δ^{13}C-OC, though, are in-line with expectations. We observed a much stronger influence of thermally labile C_4 organic matter close to the western coast of the African continent (Niger Delta (-14.0‰) and Sierra Leone Rise (-12.8‰)) compared to the more remote site in the NW Argentina Basin (-22.5‰), which were more influenced by C_3 organic matter and marine plankton sources. We note that previous studies have measured the δ^{13}C of the particulate organic matter fraction of foraminifera and have found enriched values as high as -17‰ (Hoogakker et al., 2022). Thus, apportioning the organic matter source from δ^{13}C values alone can be challenging. However, this study adds value by reporting δ^{13}C-OC values for this under-represented area.

Global climate model (GCM) simulations have suggested increases in wildfire severity and an extension of the global fire weather season, particularly in the Northwest United States and Amazonian Rainforest (de Groot et al., 2013). Additionally, GCMs have estimated an increase of elemental carbon emissions, a form of soot-like carbon using thermal optical transmittance, by 20% by the year 2050 as a result of increased wildfire burn area in the Western United States (Spracklen et al., 2009). Thus, projected future climate changes have the potential to increase carbonaceous emissions as well as mobilize soil-bound charred biomass to the ocean.

4.4 Young carbon in subtropical sediment

This study found that the particulate BC_{CTO} has a similar or greater ^{14}C fraction modern compared to the bulk TOC in subtropical Atlantic sediments. Specifically, the BC_{CTO} for the Sierra Leone Rise sediment displayed a modern age of 1030±500 ^{14}C years while the TOC had an age of 1520±200 ^{14}C years. This infers that young BC and TOC atmospheric deposition makes the organic carbon in sub-tropical Atlantic sediments vastly different compared to previous studies in the Pacific Ocean where aged BC was dominant (Coppola et al., 2014; Coppola and Druffel, 2016). Further, the radiocarbon age of atmospherically deposited bulk TOC particles on a meteorological surface buoy off the African coast was relatively modern at 2070±35 ^{14}C years, suggesting biomass burning was a large contributor to the carbon content of atmospheric particles (Eglinton et al., 2002). Similarly, $\delta^{13}C$ and $\Delta^{14}C$ values apportioned that biomass burning derived BC in sub-Saharan Africa were almost entirely from savanna grassland fires (Kirago et al., 2022).

Our radiocarbon values are consistent in that both the TOC and BC fractions were modern, suggesting little dilution by fossil fuel (radiocarbon dead) carbonaceous inputs in the surface sediments. Previous work had suggested that atmospherically transported material had a short residence time, and therefore undergoes little aging, between emission and deposition to the sediment (Raymond and Bauer, 2001; Masiello and Louchouarn, 2013). Coppola et al. (2018) also reported that BC in the Congo River displayed more modern $\Delta^{14}C$ values than other global rivers, supporting our notion of biomass-derived, e.g. young, BC particles being transported from Africa which presumably include significant fractions of subtropical C_4 grasses. The extent of

529 the young dissolved BC plume remains unclear, and whether and how it affects sedimentary BC
530 concentrations and its radiocarbon values.
531
532 Additionally, younger carbon is often thought to be more labile than radiocarbon old material
533 (Hedges et al., 1997), which suggests pelagic sediments in the subtropical Atlantic could be more
534 labile compared to the remote Pacific. The young BC radiocarbon age implies that (i) the
535 atmospheric deposition of carbon derived from biomass burning is an important transport vector
536 of organic and black carbon in the subtropical Atlantic and (ii) that minimal aging occurs
537 between atmospheric deposition to the ocean's surface and depositional flux to the deep
538 sediments.
539
540 A recent study has reported an *in situ* mechanism for the abiotic generation of ^{14}C depleted
541 graphite via hydrothermal vents (Estes et al., 2019). Previous studies have found that the
542 particulate graphite mostly settles within 200-300 m from the hydrothermal vent point source
543 (Jedwab and Boulegue, 1984). However, the submicron fraction was demonstrated to have the
544 potential for entrainment and thus could travel significant distances and be a source of aged
545 organic carbon to the deep ocean (Estes et al., 2019). While we cannot definitely conclude
546 whether the sediment samples in this study contained any graphitic BC, the relatively young ^{14}C
547 age of the BC_{CTO} sedimentary fraction would suggest minor contributions of ^{14}C depleted BC.
548 This implies that our modern ^{14}C age is a conservative estimate if any abiotic graphitic BC were
549 present in our samples.
550
551 **4. Conclusions**

552 Black carbon was ubiquitously detected in subtropical Atlantic sediments. Black carbon
553 comprised substantial fractions (17-65%) of the bulk sedimentary organic carbon, revealing that
554 terrestrial organic material composed a significant fraction of carbon present in these remote
555 region sediments. Atmospheric transport of biomass burning particulates from African grassland
556 wildfires was the most likely source for elevated black carbon concentrations (up to six times
557 greater than at a remote pelagic site) in sediment affected by the easterly trade winds. Black
558 carbon accumulation rates to subtropical Atlantic sediments ranged from 1.3±0.4 in the remote
559 Northwest Argentina Basin up to 41.6±2.2 mgBC $cm^{-2}ky^{-1}$ in the near-shore Senegal Delta.
560 Polycyclic aromatic hydrocarbon accumulation rates were lowest in the Amazon Delta (1.4±0.7
561 μgPAH $cm^{-2}ky^{-1}$) and Sierra Leone Rise (1.5±1.2 μgPAH $cm^{-2}ky^{-1}$) and greatest and most
562 variable in the Niger Delta (47.0±80.6 μgPAH $cm^{-2}ky^{-1}$) which was divergent from the BC
563 accumulation rate patterns. Lastly, the black carbon radiocarbon age, measured as the blank-
564 corrected fraction modern, was 0.95±0.01 in the Amazon Delta and 0.88±0.05 in the Sierra
565 Leone Rise. These values, compared to the total organic carbon radiocarbon blank-corrected
566 fraction modern (0.77±0.01 and 0.83±0.02, respectively), suggests the black carbon in the
567 Atlantic Ocean has a different origin and transport time compared to the Pacific Ocean and that
568 fossil carbon-derived BC input is currently minor in the subtropical Atlantic Ocean.
569

570 **Credited authorship contribution statement**

571 RL conceived this study, KAS and RL collected field samples, KAS set up and carried out
572 laboratory analyses, KAS wrote the manuscript draft, and all authors contributed to data
573 interpretation, discussions, and edits of the manuscript.
574

Declaration of competing interest

The authors declare that they have no known competing financial interests or personal relationships that could appear to influence the work reported in this paper.

Acknowledgements

This work was supported by the National Science Foundation (grant number OCE-0851044). We thank the crew, marine technicians, and captain of the *R/V Endeavor* for their help with collecting the samples. We also thank the two anonymous reviewers for their detailed review and suggestions which improved this manuscript. We acknowledge Matthias Zabel (Bremen University/ MARUM) for supplying the GeoB sediments, Ann McNichol and Mary Laudie (NOS-AMS facility at WHOI) for assistance with the radiocarbon measurements, Rick McKinney and Julia Sullivan (U.S. Environmental Protection Agency) for help with carbon analyses, Bertrand Ligouis (Tuebingen University) for petrography analyses, Torey Hart (URI) and Hilary Hamer (RPI), for help with sample collection and analysis, Rob Pockalny (URI) for help with real-time sediment core site selections for the *R/V Endeavor* cruises, and Michael St.Laurent for assistance with coding. Rainer Lohmann acknowledges a fellowship from the Hanse-WissenschaftsKolleg Delmenhorst (Germany). This document has been reviewed by the U.S. Environmental Protection Agency, Office of Research and Development, and approved for publication. The views expressed in this article are those of the authors and do not necessarily represent the views or policies of the U.S. Environmental Protection Agency. All data used in this study are provided in the Supporting Information and are available upon request. We additionally plan to upload all data to an open source repository. Views expressed in this manuscript are those of the authors and do not reflect

597 the views of the National Oceanic and Atmospheric Administration or the Department of
598 Commerce.
599
600 **References**

601 Accardi-Dey, A., & Gschwend, P. M. (2002), Assessing the combined roles of natural organic
602 matter and black carbon as sorbents in sediments, *Environ Sci Technol*, *36*(1), 21-29.
603 Adhikari, P. L., Maiti, K., Overton, E. B., Rosenheim, B. E., & Marx, B. D. (2016). Distributions
604 and accumulation rates of polycyclic aromatic hydrocarbons in the northern Gulf of
605 Mexico sediments. *Environmental pollution*, *212*, 413-423.
606 Andreae, M. O. (1993). The influence of tropical biomass burning on climate and the
607 atmospheric environment. *In Biogeochemistry of Global Change: Radiatively Active*
608 *Trace Gases Selected Papers from the Tenth International Symposium on Environmental*
609 *Biogeochemistry*, San Francisco, August 19–24, 1991 (pp. 113-150). Springer US.
610 Bond, T. C., & Sun, H., (2005), Can reducing black carbon emissions counteract global
611 warming?, *Environmental Science & Technology*, 39.16, 5921-5926.
612 Burke, A., Robinson, L.F., McNichol, A.P., Jenkins, W.J., Scanlon, K.M., & Gerlach, D.S.,
613 (2010), Reconnaissance dating: a new radiocarbon method applied to assessing the
614 temporal distribution of Southern Ocean deep-sea corals, *Deep Sea Research Part I:*
615 *Oceanographic Research Papers*, 57, no. 11, 1510-1520.
616 Cahoon, D. R., Stocks, B. J., Levine, J. S., Cofer, W. R., & O'Neill, K. P. (1992), Seasonal
617 Distribution of African Savanna Fires, *Nature*, *359*(6398), 812-815.

618 Carvalho, F. P., Oliveira, J.M., & Soares, A.M.M. (2011), Sediment accumulation and
619 bioturbation rates in the deep Northeast Atlantic determined by radiometric techniques,
620 *ICES J. Mar. Sci.*, 68 (3), 427-435
621 Cerling, T. E., Wang, Y., & Quade, J. (1993). Expansion of C4 ecosystems as an indicator of
622 global ecological change in the late Miocene. Nature, 361(6410), 344-345.
623 Coppola, A. I., Wagner, S., Lennartz, S. T., Seidel, M., Ward, N. D., Dittmar, T., ... & Jones, M.
624 W. (2022). The black carbon cycle and its role in the Earth system. *Nature Reviews Earth*
625 *& Environment*, *3*(8), 516-532.
626 Coppola, A. I., Ziolkowski, L. A., Masiello, C.A., & Druffel, E. R. M.. (2014) Aged black
627 carbon in marine sediments and sinking particles. *Geophysical Research Letters* 41(7):
628 2427-2433.
629 Coppola, A. I., & Druffel, E. R. (2016). Cycling of black carbon in the ocean. *Geophysical*
630 *Research Letters*, *43*(9), 4477-4482.
631 Coppola, A.I., Wiedemeier, D.B., Galy, V., Haghipour, N., Hanke, U.M., Nascimento, G.S.,
632 Usman, M., Blattmann, T.M., Reisser, M., Freymond, C.V. and Zhao, M., (2018).
633 Global-scale evidence for the refractory nature of riverine black carbon. *Nature*
634 *Geoscience*, p.1.
635 Crelling J., Huggett, W., Borrego, A.G., Hower, J., Ligouis, B., Mastalerz, M., Misz, M., Suárez-
636 Ruiz, I., & Valentim, B. (2006), International Committee for Coal and Organic Petrology
637 (ICCP), Atlas of anthropogenic particles: Indiana Geological Survey Open-File Study 06-
638 01, CD-ROM.
639 Currie, L. A., Benner, B. A., Kessler, J. D., Klinedinst, D. B., Klouda, G. A., Marolf, J. V.,

Slater, J. F., Wise, S. A., Cachier, H., Cary, R., Chow, J. C., Watson, J., Druffel, E. R. M., Masiello, C. A., Eglinton, T. I., Pearson, A., Reddy, C. M., Gustafsson, O., Quinn, J. G., Hartmann, P. C., Hedges, J. I., Prentice, K. M., Kirchstetter, T. W., Novakov, T., Puxbaum, H., & Schmid, H. (2002), A critical evaluation of interlaboratory data on total, elemental, and isotopic carbon in the carbonaceous particle reference material, NIST SRM 1649a, *Journal of Research of the National Institute of Standards and Technology*, 107, 279–298.

Dickens, A. F., Gelinas, Y., Masiello, C. A., Wakeham, S., & Hedges, J. I. (2004), Reburial of fossil organic carbon in marine sediments, *Nature*, *427*(6972), 336-339.

De Groot, W. J., Flannigan, M. D., & Stocks, B. J. (2013). Climate Change and Wildfires. *In Proceedings of the Fourth International Symposium on Fire Economics, Planning, and Policy: Climate Change and Wildfires.* Notes. Mexico (pp. 1-10).

Eglinton, T. I., Eglinton, G., Dupont, L., Sholkovitz, E. R., Montluçon, D., & Reddy, C.M.. (2002), Composition, age, and provenance of organic matter in NW African dust over the Atlantic Ocean. *Geochemistry, Geophysics, Geosystems,* 3, no. 8, 1-27.

Elmquist, M., Gustafsson, O., & Andersson, P. (2004), Quantification of sedimentary black carbon using the chemothermal oxidation method: an evaluation of ex situ pretreatments and standard additions approaches, *Limnol Oceanogr-Meth*, *2*, 417-427.

Elum, Z. A., Mopipi, K., & Henri-Ukoha, A. (2016). Oil exploitation and its socioeconomic effects on the Niger Delta region of Nigeria. *Environmental Science and Pollution Research*, 23, 12880-12889.

661 Estes, E. R., Berti, D., Coffey, N. R., Hochella Jr, M. F., Wozniak, A. S., & Luther III, G. W.
662 (2019). Abiotic synthesis of graphite in hydrothermal vents. Nature
663 Communications, 10(1), 5179.
664 Farquhar, G. D., Ehleringer, J. R., & Hubick, K. T. (1989). Carbon isotope discrimination and
665 photosynthesis. Annual review of plant biology, 40(1), 503-537.
666 Forbes, M. S., Raison, R. J., & Skjemstad, J. O. (2006). Formation, transformation and transport
667 of black carbon (charcoal) in terrestrial and aquatic ecosystems. Science of the total
668 environment, 370(1), 190-206.
669 Goldberg, E. D. (1985), Black Carbon in the Environment, *Wiley, New York*.
670 Griffin, J. J. & Goldberg, E. D., (1975) The fluxes of elemental carbon in coastal marine
671 sediments. *Limnol. Oceanogr*. 20: 256–263.
672 Gustafsson, O., F. Haghseta, C. Chan, J. MacFarlane, and P. M. Gschwend (1997),
673 Quantification of the dilute sedimentary soot phase: Implications for PAH speciation and
674 bioavailability, *Environ Sci Technol*, *31*(1), 203-209.
675 Gschwend, P. M., & Hites, R. A. (1981). Fluxes of polycyclic aromatic hydrocarbons to marine
676 and lacustrine sediments in the northeastern United States. *Geochimica et Cosmochimica*
677 *Acta*, *45*(12), 2359-2367.
678 Gysel, M., Laborde, M., Olfert, J. S., Subramanian, R., & Grohn, A. J. (2011), Effective density
679 of Aquadag and fullerene soot black carbon reference materials used for SP2 calibration,
680 *Atmospheric Measurement Techniques*, 4, 2851-2828.
681 Hammes, K., et al. (2007), Comparison of quantification methods to measure fire-derived
682 (black/elemental) carbon in soils and sediments using reference materials from soil,
683 water, sediment and the atmosphere, *Global Biogeochem Cy*, *21*(3).

Hedges, J. I., Keil, R. G., & Benner, R. (1997), What happens to terrestrial organic matter in the ocean?, *Org Geochem*, *27*(5-6), 195-212.

Holtvoeth, J., Wagner, T., & Schubert, C. J. (2003), Organic matter in river-influenced continental margin sediments: The land-ocean and climate linkage at the Late Quaternary Congo fan (ODP Site 1075), *Geochem Geophy Geosy*, *4*.

Hoogakker, B. A., Anderson, C., Paoloni, T., Stott, A., Grant, H., Keenan, P., ... & Peck, V. L. (2022). Planktonic foraminifera organic carbon isotopes as archives of upper ocean carbon cycling. Nature communications, 13(1), 4841.

Jedwab, J., & Boulègue, J. (1984). Graphite crystals in hydrothermal vents. Nature, 310(5972), 41-43.

Kirago, L., Gatari, M. J., Gustafsson, Ö., & Andersson, A. (2022a). Black carbon emissions from traffic contribute substantially to air pollution in Nairobi, Kenya. *Communications Earth & Environment*, 3(1), 74.

Kirago, L., Gustafsson, O., Gaita, S. M., Haslett, S. L., deWitt, H. L., Gasore, J., ... & Andersson, A. (2022b). Atmospheric Black Carbon Loadings and Sources over Eastern Sub-Saharan Africa Are Governed by the Regional Savanna Fires. *Environmental Science & Technology*, 56(22), 15460-15469.

Kuhlbusch, T. A. J., & Crutzen, P. J. (1995), Toward a global estimate of black carbon in residues of vegetation fires representing a sink of atmospheric CO_2 and a source of O_2, Global Biogeochemical Cycles, 9, no. 4, 491-501.

Kuhlbusch, T. A. J., (1998), Enhanced: Black carbon and the carbon cycle, *Science*, 280, no. 5371, 1903-1904.

Li, Y., Henze, D. K., Jack, D., Henderson, B. H., & Kinney, P. L., (2016), Assessing public health burden associated with exposure to ambient black carbon in the United States, *Science of The Total Environment*, 539, 515-525.

Lohmann, R., Bollinger, K., Cantwell, M., Feichter, J., Fischer-Bruns, I., & Zabel, M. (2009), Fluxes of soot black carbon to South Atlantic sediments, *Global Biogeochem Cy*, *23*.

Masiello, C. A. (2004), New directions in black carbon organic geochemistry, *Mar Chem*, *92*(1-4), 201-213.

Masiello, C. A., & Druffel, E. R. M. (1998), Black carbon in deep-sea sediments, *Science*, *280*(5371), 1911-1913.

Masiello, C. A., & Louchouarn, P. (2013), Fire in the Ocean, *Science*, *340*(6130), 287-288.

McIntyre, C. P., Roberts, M.L., Burton, J.R., McNichol, A.P., Burke, A., Robinson, L.F., von Reden, K.F., & Jenkins, W.J. (2011). Rapid radiocarbon (^{14}C) analysis of coral and carbonate samples using a continuous-flow accelerator mass spectrometry (CFAMS) system, *Paleoceanography* 26, no. 4.

Middelburg, J. J., Nieuwenhuize, J., & van Breugel, P. (1999). Black carbon in marine sediments. *Marine Chemistry*, *65*(3-4), 245-252.

Mitra, S., Zimmerman, A.R., Hunsinger, G.B., & Woerner, W.R. (2014), Black carbon in coastal and large river systems, Biogeochemical Dynamsics at Major River-Coastal Interfaces-Linkages with Climate Change., edited by Thomas S. Bianchi., Mead A. Allison, Wei-Jun Cai. Cambridge University Press, New York, NY, USA. pp. 200-234.

Pikkarainen, A. L. (2004). Polycyclic aromatic hydrocarbons in Baltic Sea sediments. *Polycyclic Aromatic Compounds*, *24*(4-5), 667-679.

729 Perry, K. D., Cahill, T. A., Eldred, R. A., Dutcher, D. D., & Gill, T. E. (1997), Long-range
730 transport of North African dust to the eastern United States. *Journal of Geophysical*
731 *Research: Atmospheres*, 102(D10), 11225-11238.
732 Pohl, K., Cantwell, M., Herckes, P., & Lohmann, R. (2014), Black carbon concentrations and
733 sources in the marine boundary layer of the tropical Atlantic ocean using four
734 methodologies, *Atmospheric Chemistry and Physics*, 14, 7431-7443.
735 Raymond, P. A., & Bauer, J. E. (2001), Riverine export of aged terrestrial organic matter to the
736 North Atlantic Ocean, *Nature*, *409*(6819), 497-500.
737 Sánchez-García, L., Cato, I., & Gustafsson, Ö. (2012). The sequestration sink of soot black
738 carbon in the Northern European Shelf sediments. *Global Biogeochemical*
739 *Cycles*, *26*(1).
740 Schmidt, M. W. I., & Noack, A. G. (2000), Black carbon in soils and sediments: Analysis,
741 distribution, implications, and current challenges, *Global Biogeochem Cy*, *14*(3), 777-
742 793.
743 *Schmittner, A., Bostock, H. C., Cartapanis, O., Curry, W. B., Filipsson, H. L., Galbraith, E. D.,*
744 *... & Waelbroeck, C. (2017). Calibration of the carbon isotope composition (δ13C) of*
745 *benthic foraminifera. Paleoceanography, 32(6), 512-530.*
746 Seiler, W., & Crutzen, P. J. (1980), Estimates of Gross and Net Fluxes of Carbon between the
747 Biosphere and the Atmosphere from Biomass Burning, *Climatic Change*, *2*(3), 207-247.
748 Spracklen, D. V., Mickley, L. J., Logan, J. A., Hudman, R. C., Yevich, R., Flannigan, M. D., &
749 Westerling, A. L. (2009). Impacts of climate change from 2000 to 2050 on wildfire
750 activity and carbonaceous aerosol concentrations in the western United States. *Journal of*
751 *Geophysical Research: Atmospheres*, 114(D20).

St Laurent, K. A., Hribar, D. J., Carlson, A. J., Crawford, C. M., & Siok, D. (2020). Assessing coastal carbon variability in two Delaware tidal marshes. *Journal of Coastal Conservation*, *24*(6), 1-16.

Suman, D. O., Kuhlbusch, T. A. J., & Lim, B. (1997), Marine Sediments: A reservoir for black carbon and their use as spatial and temporal records of combustion, *Sediment Records of Biomass Burning and Global Change*, *edited by J. S. Clark, H. Cachier, J. G. Goldhammer, B. J. Stocks* (Springer-Verlag).

Taylor, G. H., Teichmüller, M., A., D., Diessel, C.F.K., Littke, R., & Robert, P. (1998), Organic Petrology. Gebrüder Bornträger, Berlin-Stuttgart, 704p.

Teal, L. R., Mark T. Bulling, E. R. Parker, and Martin Solan. (2008) "Global patterns of bioturbation intensity and mixed depth of marine soft sediments." *Aquatic Biology* 2, no. 3: 207-218.

www.pangaea.de, Data Publisher for Earth & Environmental Science, accessed summer 2012.

Wagner, T., Zabel, M., Dupont, L., Holtvoeth, J., & Schubert, C.J. (2004). "Terrigenous signals in sediments of the low latitude Atlantic—implications for environmental variations during the Late Quaternary, Part I: organic carbon." *The South Atlantic in the late Quaternary:* Reconstruction of material budgets and current systems: Berlin, Springer,

Xu, X. M., Trumbore, S.E., Zheng, S.H., Southon, J.R., McDuffee, K.E., Luttgen, M., & Liu, J.C., (2007), Modifying a sealed tube zinc reduction method for preparation of AMS graphite targets: Reducing background and attaining high precision, *Nucl. Instrum. Methods Phys. Res.*, Sect. B, 259(1).

Yeh, H. W., & Epstein, S. (1981). Hydrogen and carbon isotopes of petroleum and related organic matter. Geochimica et Cosmochimica Acta, 45(5), 753-762.

775 Yunker, M. B., Macdonald, R. W., Vingarzan, R., Mitchell, R. H., Goyette, D., & Sylvestre, S.
776 (2002). PAHs in the Fraser River basin: a critical appraisal of PAH ratios as indicators of
777 PAH source and composition. *Organic geochemistry*, *33*(4), 489-515.
778 Zabel, M., Wagner, T., & deMenocal, P. (2003), Terrigenous signals in sediments of the low-
779 latitude Atlantic- Indications to environmental variations during the Late Quarternary,
780 part II: Lithogenic Matter *The South Atlantic in the Late Quarternary: Reconstruction of*
781 *the Material Budgets and Current Systems* 323-345.
782

Table 1

Surface sediment concentrations ($g_C\ kg_{sed}^{-1}$ ***) of black carbon (*** BC_{CTO}***;*** $BC_{optical}$***), organic carbon (OC), total organic carbon (TOC) and the ratio of*** BC_{CTO} ***to TOC in subtropical Atlantic sediments.***

	Concentration ($g_C\ kg_{sed}^{-1}$)				
Regional Average	**TOC**	**BC_{CTO}**	**OC_{CTO}**	**$BC_{optical}$**	**BC_{CTO}/TOC**
Amazon Basin	6.4±1.8 (n=45)	4.1±1.4 (n=48)	2.3±1.4 (n=45)	4-17 (n=3)	0.65±0.18 (n=45)
Niger Delta	15.9±6.1 (n=77)	7.4±2.4 (n=77)	8.4±8.0 (n=75)	n/a	0.56±0.26 (n=75)
Senegal Delta	22.0±1.0 (n=6)	7.7±0.4 (n=6)	14.4±0.8 (n=6)	n/a	0.35±0.01 (n=6)
Sierra Leone Rise	15.4±3.4 (n=58)	6.5±3.1 (n=64)	8.9±4.2 (n=53)	5-18 (n=2)	0.44±0.20 (n=53)
NW Argentina Basin	7.0±0.9 (n=10)	1.1±0.3 (n=8)	5.8±1.1 (n=8)	n/a	0.17±0.06 (n=8)

Table 2

Estimated literature-derived sedimentation rates (cm kyr^{-1}) and black carbon (mgBC cm^{-2} kyr^{-1}) and polycyclic aromatic hydrocarbon (μgPAH cm^{-2} kyr^{-1}) accumulation (Acc.) rates to subtropical Atlantic sediments.

Region	Sedimentation Rate (cm kyr^{-1})	BC Acc. Rate (mgBC cm^{-2} kyr^{-1})		PAH Acc. Rate (μgPAH cm^{-2} kyr^{-1})
		BC$_{optical}$	**BC$_{CTO}$**	
Amazon Delta	~1.3	2.8-12.1; n=3	2.9±1.0; n=48	1.4±0.7; n=19
Niger Delta	~10	n/a	24.6±8.0; n=77	47.0±80.6; n=38
Senegal Delta	~6.9	n/a	41.6±2.2; n=6	20.9±12.5; n=3
Sierra Leone Rise	~2.7	6.6-23.8; n=2	8.4±4.1; n=64	1.5±1.2; n=18
NW Argentina Basin	~2.5	n/a	1.3±0.4; n=8	4.5±4.8; n=5

Table 3

Stable carbon (δ^{13}C), radiocarbon carbon (Δ^{14}C), and polycyclic aromatic hydrocarbon (PAH) ratios and concentrations in subtropical Atlantic sediments.

	‰		Fraction Modern (FM$_c$)		μgPAH g$_{sed}^{-1}$			
Regional Average	**δ^{13}C$_{TOC}$**	**δ^{13}C$_{BC}$**	**Δ^{14}C$_{TOC}$**	**Δ^{14}C$_{BC}$**	**∑PAHs**	**IP/(IP+Bghi)**	**Fl/(Fl+Py)**	**An/178**
Amazon Delta	-20.3±1.7; n=45	-28.3±4.6; n=48	0.77±0.01; n=5	0.95±0.01; n=5	1.93±0.94; n=19	0.55±0.23	0.71±0.22	0.56±0.33
Niger Delta	-19.2±1.1; n=75	-23.9±4.6; n=77	n/a	n/a	14.12±24.21; n=38	0.32±0.30	0.55±0.15	0.45±0.27
Senegal Delta	-19.7±0.1; n=6	-21.2±3.1; n=6	n/a	n/a	3.87±2.31; n=3	0.71±0.11	0.59±0.05	0.27±0.02
Sierra Leone Rise	-17.2±1.2; n=57	-23.2±4.6; n=63	0.83±0.02; n=5	0.88±0.05; n=4	1.13±0.89; n=18	0.42±0.13	0.71±0.07	0.35±0.13
NW Argentina Basin	-22.6±0.9; n=10	-25.4±1.5; n=8	n/a	n/a	3.84±4.05; n=5	0.88±0.21	0.10±0.03	0.84±0.06

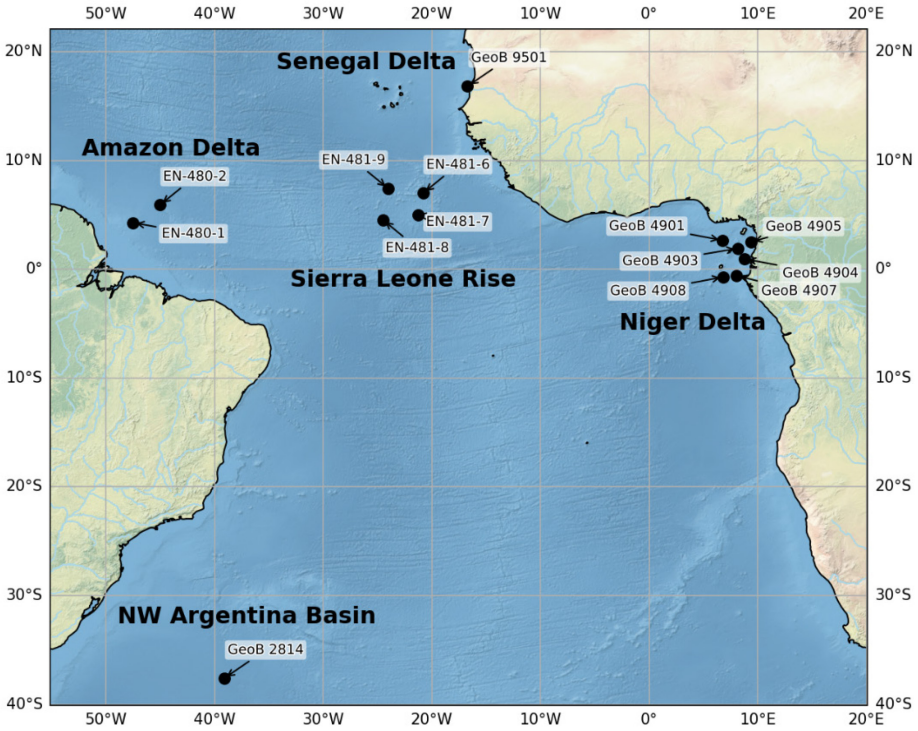

804

805 **Figure 1.** Sediment sample locations and regions.

806

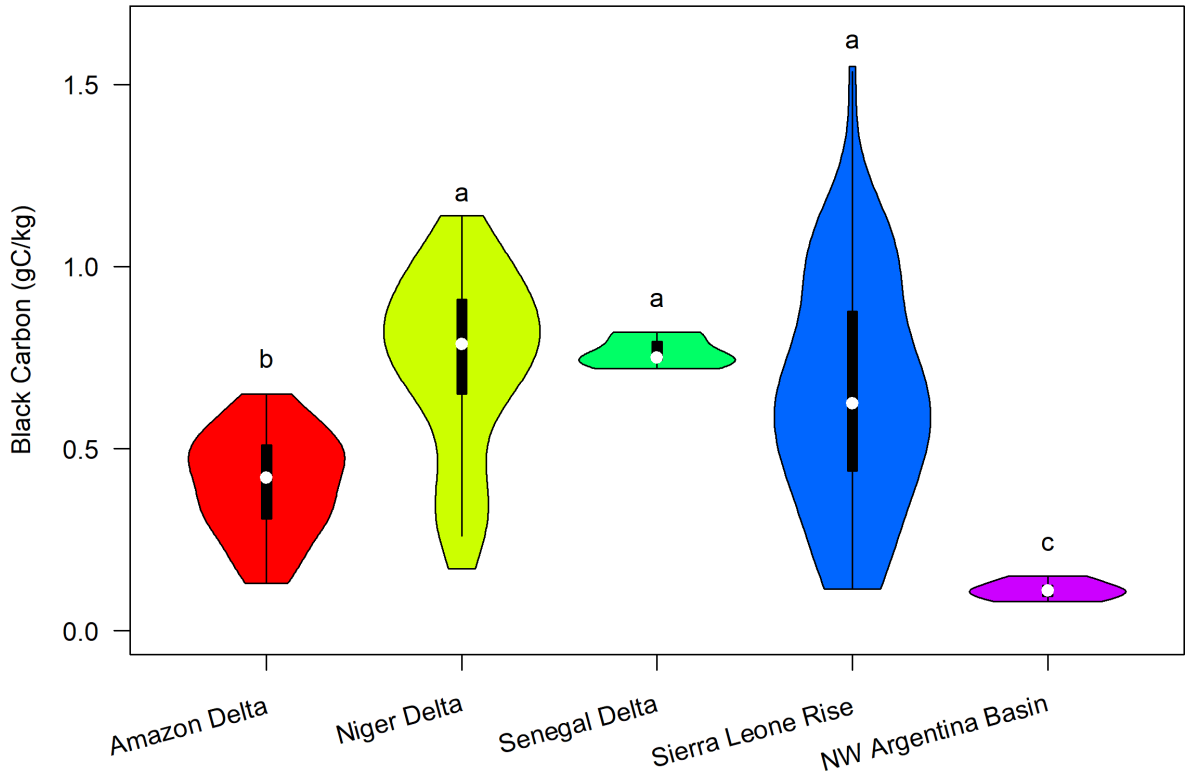

807

808 **Figure 2.** Subtropical Atlantic average BC_{CTO} surface sediment concentration by region. A

809 compressed letter display denotes whether regions where significantly different.

810

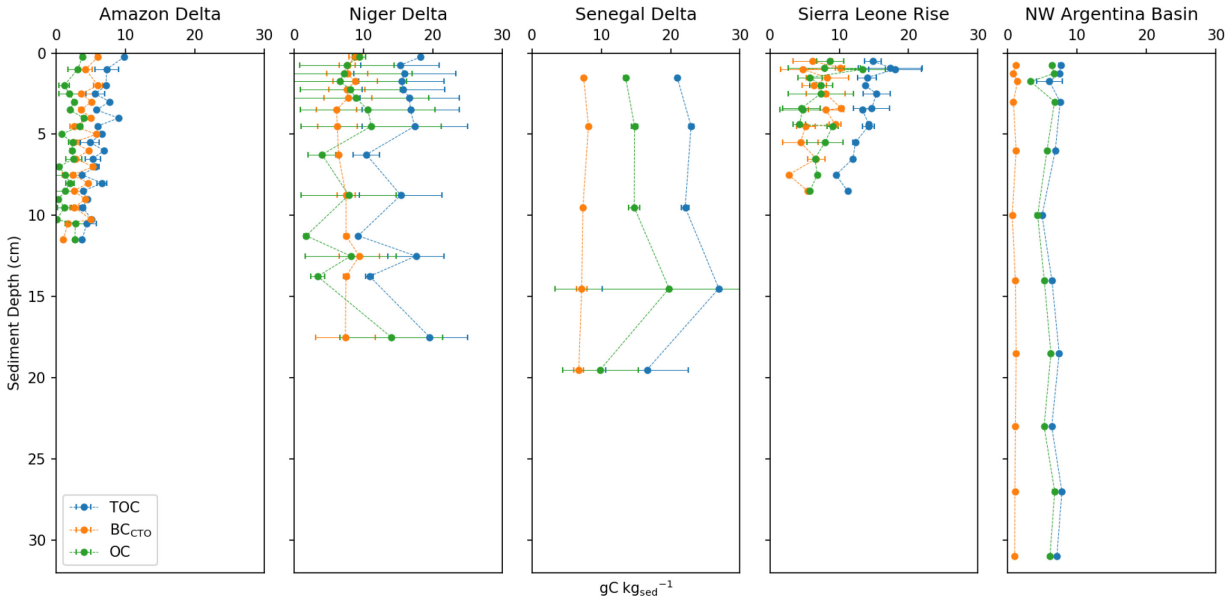

811

812 **Figure 3.** Upcore BC_{CTO}, OC, and TOC concentrations. Y-axis is centimeters below seafloor.
813 Data were aggregated by region and averaged by sediment depth.

814

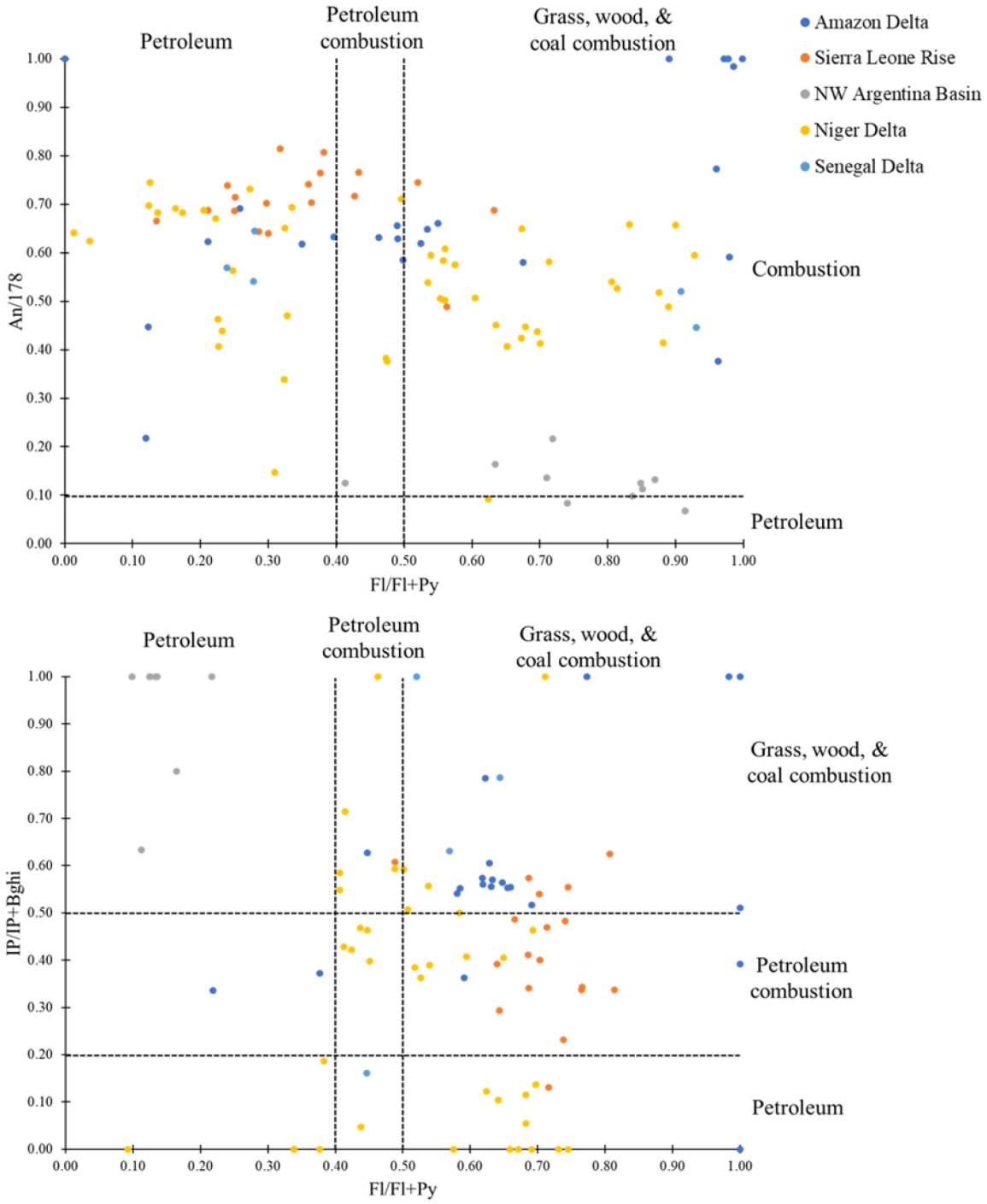

Figure 4. Source apportionment estimates using the ratios of select polycyclic aromatic hydrocarbons (Anthracene (An), Pyrene (Py), Fluoranthene (Fl), Benzo(g,h,i)perylene (Bghi), Indeno(1,2,3-c,d)pyrene (IP), and 178 (sum of Phenanthrene and An) as described by Yunker al., 2002.